Coordinated control of on-load tap changer and energy storage systems for voltage support in distribution networks

Antonio Giannitrapani, Simone Paoletti, Antonio Vicino, Donato Zarrilli

***Abstract*— The use of energy storage systems is widely recognized as a key tool to create a more resilient energy infrastructure. At the same time, new technologies such as soft-open points and on-load tap changers are deserving growing attention for their potential applications in smart grids. In this paper we consider the coordinated use of on-load tap changer and energy storage systems for voltage support in distribution networks. We first formulate the optimal control problem over a given time horizon as a multi-period optimal power flow. To cope with uncertainties such as inaccurate forecasts, the optimal control problem is then inserted into a receding horizon scheme. The proposed approach requires very limited information to predict possible voltage problems and counteract them in advance. The control algorithm is tested on real data from a low voltage network featuring over- and undervoltages in the absence of voltage control. The obtained results show that the coordinated use of on-load tap changer and storage devices allows one to dramatically reduce the size of the installed storage units required to alleviate voltage issues.**

I. Introduction

While on-load tap changers (OLTCs) have been used since long time at primary substations to regulate voltage, only recently the increasing automation of distribution networks has made it possible to use OLTC-fitted transformers in secondary substations, especially in urban areas. This motivates the current interest of researchers in OLTC control algorithms for applications in distribution networks. Indeed, several approaches exploiting OLTC can be found in the literature [1], often focused on control strategies integrating the operation of OLTC-fitted transformers with other controllable devices [2], [3], [4]. This is done in order to deal with practical limitations on the frequency and magnitude of tap changes. Moreover, the OLTC is ineffective in case over- and undervoltages occur at the same time.

Another technology which is becoming more and more frequent in distribution networks is energy storage. Energy storage systems (ESSs) are nowadays recognized as fundamental elements for the transition to the smart grid, in view of the numerous benefits they bring, both to the power system and its stakeholders [5]. A large body of literature deals with the problem of ESS allocation [6], i.e. deciding the optimal ESS number, locations and sizes to attain a given control objective. However, if uncertainties at the planning stage are not properly considered, it might not be possible in practice to operate the ESSs while satisfying power quality specifications. Coordinated solutions involving ESSs and OLTC could then be used to robustify the overall control strategy [7], [8].

In [9] we addressed ESS operation for voltage support in distribution networks within a receding horizon framework. In this paper we extend our previous work by considering the coordinated use of OLTC and ESSs. We first formulate the optimal control problem over a given time horizon as a multi-period AC optimal power flow (M-OPF). The formulated problem includes the dynamics of the voltage at the bus where the OLTC is installed, and penalizes its use in the objective function. Since forecasts of demand and generation are needed for the M-OPF problem, and the available on-line measurements are limited to the MV/LV substation, a simple forecasting approach is adopted, similar to the one proposed in [9]. To cope with inaccurate forecasts and other uncertainties, the optimal control problem is integrated into a receding horizon scheme, where at each time step the M-OPF problem is solved, and only the first control action is applied to both the OLTC and the ESSs. An attractive feature of the proposed approach is the limited information required to predict possible voltage problems and counteract them in advance through suitable OLTC and ESS control policies.

The paper is organized as follows. Section II describes the bus injection model of a LV network equipped with OLTC and ESSs. The M-OPF for optimal coordinated OLTC-ESS control is presented in Section III, and its receding horizon implementation, including the approach used for demand and generation forecasting, is summarized in Section IV. Section V reports numerical results obtained using data from a real Italian LV network. Finally, conclusions are drawn in Section VI.

II. Network model

In this section, the model of a distribution network including loads, distributed generators, ESSs and OLTC is introduced (e.g., see [10, Chap. 9]). The following notation is used in the remainder of the paper. The real part, imaginary part and complex conjugate of a complex number $z \in \mathbb{C}$ are denoted by $\mathrm{Re}(z)$, $\mathrm{Im}(z)$ and z^*, respectively. For a fixed sampling time ΔT, the value of a variable x at time $t\Delta T$ is denoted by $x(t)$, where $t = 1, 2, \ldots$ is the discrete time index. The h-step ahead forecast of the variable x, based on the information available up to time t, is denoted by $\hat{x}(t+h|t)$, where h is a positive integer.

An LV network can be represented by a graph $(\mathcal{N}, \mathcal{E})$, where $\mathcal{N} = \{1, 2, \ldots, n\}$ is the set of nodes (corresponding to the network *buses*) and $\mathcal{E}$ is the set of edges (corresponding

The authors are with the Dipartimento di Ingegneria dell'Informazione e Scienze Matematiche, Università degli Studi di Siena, Siena 53100, Italy (e-mail: giannitrapani@dii.unisi.it; paoletti@dii.unisi.it; vicino@dii.unisi.it; zarrilli@dii.unisi.it).

to the network *lines*). Bus 1 is assumed to be the slack bus, representing the interconnection with the MV network, while the set $\mathcal{N}^L = \{2, \dots, n\}$ includes all the remaining buses. The complex voltage at bus k is denoted by V_k. Typical specifications on the voltage quality require that the voltage magnitude at all buses is kept within specified limits, i.e.

$$\underline{v}_k^2 \leq |V_k(t)|^2 \leq \overline{v}_k^2, \tag{1}$$

where $0 < \underline{v}_k \leq \overline{v}_k$ are given bounds. Conventionally, the phase of the voltage $V_1(t)$ is set to zero for all t. When the MV/LV substation is equipped with OLTC, the voltage magnitude at the slack bus can be modified by changing the transformation ratio. In this case, the dynamics of the slack bus voltage can be modeled as

$$V_1(t+1) = V_1(t) + l(t), \tag{2}$$

where $l(t) \in \mathbb{R}$ denotes the voltage increment resulting from the OLTC action. In practice, the voltage variation that can be executed in the time interval ΔT is bounded, i.e.

$$|l(t)|^2 \leq \overline{l}^2, \tag{3}$$

where the bound $\overline{l} > 0$ depends on the OLTC technology and the sampling time ΔT.

Let $\mathcal{S} \subseteq \mathcal{N}^L$ be the set of buses equipped with ESSs. For $s \in \mathcal{S}$, $e_s(t)$ denotes the storage energy level at bus s and time t. It is bounded as follows:

$$0 \leq e_s(t) \leq E_s, \tag{4}$$

where E_s is the storage capacity installed at bus s. The dynamics of $e_s(t)$ is standard [11], and modelled by the first-order difference equation

$$e_s(t+1) = e_s(t) + \eta_s^c r_s^c(t)\Delta T - \frac{1}{\eta_s^d} r_s^d(t)\Delta T, \tag{5}$$

where $r_s^c(t) \geq 0$ and $r_s^d(t) \geq 0$ are the average active power pumped into and drawn from the storage between t and $t+1$, respectively, and $\eta_s^c, \eta_s^d \in (0, 1]$ represent the charging and discharging efficiencies of the ESS at bus s. Since an ESS cannot be simultaneously charged and discharged, the following complementarity constraints holds

$$r_s^c(t) r_s^d(t) = 0. \tag{6}$$

Let $r_s(t)$ and $b_s(t)$ be the average active and reactive power exchanged by the storage at bus s between time t and $t+1$, respectively. Notice that $r_s(t)$ can be written as

$$r_s(t) = r_s^c(t) - r_s^d(t). \tag{7}$$

Bounds on the maximum active and reactive power exchanged by the ESSs can be imposed as

$$M_s \begin{bmatrix} r_s(t) \\ b_s(t) \end{bmatrix} \leq m_s, \tag{8}$$

where $M_s \in \mathbb{R}^{p \times 2}$ and $m_s \in \mathbb{R}^p$. Notice that the constraint formulation (8) is quite general, forcing the active and reactive power to lie in a convex polytope. In particular, this allows one to express possible coupling existing among the active and reactive power bounds [12].

Let $y_{ij} = y_{ji}$ be the line admittance between nodes i and j, with the convention that $y_{ij} = 0$ if $(i, j) \notin \mathcal{E}$. Moreover, let y_{ii} denote the admittance-to-ground at bus i. The network admittance matrix $Y = [Y_{ij}] \in \mathbb{C}^{n \times n}$ is a symmetric matrix defined as

$$Y_{ij} = \begin{cases} y_{ii} + \sum_{h \neq i} y_{ih} & \text{if } i = j \\ -y_{ij} & \text{otherwise.} \end{cases} \tag{9}$$

The physical properties of the lines constrain the admissible values of real power flow from bus i to bus j, i.e.

$$\mathrm{Re}\big(V_i(t)\big[V_i(t) - V_j(t)\big]^* y_{ij}^*\big) \leq \overline{P}_{ij}, \tag{10}$$

where $\overline{P}_{ij} = \overline{P}_{ji}$ is a given upper bound. Denoting the active and reactive power injections at bus k by P_k and Q_k, respectively, the power balance equations at bus k and time t read as

$$P_k(t) = \mathrm{Re}\Big(V_k(t) \sum_{j \in \mathcal{N}} V_j^*(t) Y_{kj}^*\Big) \tag{11a}$$

$$Q_k(t) = \mathrm{Im}\Big(V_k(t) \sum_{j \in \mathcal{N}} V_j^*(t) Y_{kj}^*\Big). \tag{11b}$$

If a bus k is equipped with loads, generators and ESS, P_k and Q_k can be decomposed as

$$P_k(t) = P_k^G(t) - P_k^D(t) - r_k(t-1) \tag{12a}$$

$$Q_k(t) = Q_k^G(t) - Q_k^D(t) - b_k(t-1), \tag{12b}$$

where the superscript ^{G} refers to generation and the superscript ^{D} refers to demand. Notice that, following the convention adopted in power systems, measurements of average power are labeled a posteriori, i.e., the power ascribed at time t represents the average power between $t-1$ and t. On the other hand, the ESS control inputs holding between $t-1$ and t are denoted by $r_k(t-1)$ and $b_k(t-1)$, consistently with the fact that they are decided at time $t-1$. Putting together (11) and (12), we get

$$\mathrm{Re}\Big(V_k(t) \sum_{j \in \mathcal{N}} V_j^*(t) Y_{kj}^*\Big) = P_k^G(t) - P_k^D(t) - r_k(t-1) \tag{13a}$$

$$\mathrm{Im}\Big(V_k(t) \sum_{j \in \mathcal{N}} V_j^*(t) Y_{kj}^*\Big) = Q_k^G(t) - Q_k^D(t) - b_k(t-1). \tag{13b}$$

Active power $P_1(t)$ and reactive power $Q_1(t)$ injected at the slack bus are determined by the power flow equations. For all other buses in the set $\mathcal{N}^L$, $V_k(t)$ are free variables of the power flow problem, while the quantities $P_k^D(t)$, $Q_k^D(t)$, $P_k^G(t)$ and $Q_k^G(t)$ are considered as known inputs in (13). In case no load or generator is connected to bus k, the corresponding demand or generation are assumed to be zero. Similarly, if a bus is not equipped with an ESS, the corresponding active and reactive power is zero, i.e. $r_k(t-1) = b_k(t-1) = 0$ for $k \in \mathcal{N}^L \backslash \mathcal{S}$.

III. Coordinated OLTC-ESS control

In this section, we show how to formulate the integrated control of ESSs and OLTC as an optimization problem. At time t, the amount of active and reactive power exchanged by each ESS, as well as the voltage variation at the slack bus implemented by the OLTC, are computed by solving a suitable optimal control problem over the time horizon $\mathcal{T} = \{t+1, \dots, t+H\}$, where the parameter $H > 0$ represents the length of the control horizon. In the design of a network operation policy, several objectives have to be taken into account. Minimizing line losses is of paramount importance, since the losses at distribution level represent the majority of the total losses in the grid. Another aspect to be considered is the deterioration of the ESSs, which depends on the ESS usage and state of charge (SoC). Similarly, the OLTC device should be used as little as possible in order to minimize the wear of the transformer and prolong its lifespan. These considerations lead to the following cost function associated to a single time period t

$$C(t) = C_L(t) + \gamma_S C_S(t) + \gamma_O C_O(t), \tag{14}$$

where $\gamma_S \geq 0$ and $\gamma_O \geq 0$ are suitable weights. The term

$$C_L(t) = \sum_{k \in \mathcal{N}} P_k(t) \Delta T \tag{15}$$

represents the total real losses in the network between $t-1$ and t, whereas

$$C_S(t) = \sum_{s \in \mathcal{S}} \big(r_s^c(t-1) + r_s^d(t-1) \big) \Delta T \tag{16}$$

is a measure of the battery usage over the same time period. Similarly, the term

$$C_O(t) = |l(t)|^2 \tag{17}$$

is used to penalize OLTC actions. An additional cost $C_T(t)$ can be included in order to weight deviations of the ESS SoC from a desired level:

$$C_T(t) = \sum_{s \in \mathcal{S}} \big| e_s(t) - \xi E_s \big|, \tag{18}$$

where $\xi \in [0,\ 1]$ represents the desired SoC.

At time t, the objective is to find an ESS and OLTC control policy such that the total cost over the control horizon $\mathcal{T}$ is minimized, while satisfying voltage quality and power flow constraints, and OLTC and ESS specifications. This translates into the multi-period OPF problem (19), where $\gamma_T \geq 0$ is a parameter determining the relative importance of the cost $C_T(t+H)$ on the terminal state with respect to the sum of the instantaneous costs $C(t)$ over the horizon $\mathcal{T}$. The purpose of the term $\gamma_T C_T(t+H)$ is to drive the SoC at the end of the control horizon towards the target ξ, compatibly with the voltage quality and power flow constraints.

Problem (19) is nonconvex, due to the power flow constraints (10), the power balance equations (13), and the complementarity constraint (6) on the ESS charging and discharging control inputs. A possible approach is to solve a suitable convex relaxation of (19), and verify a posteriori the feasibility of the obtained solution for the original problem. A recent method to cope with nonconvex constraints (10) and (13) is to formulate the OPF problem as an SDP problem which, after removing a rank-1 condition, provides a convex relaxation of (19) (e.g., see [13], [14], [15]). This approach is known to work particularly well for OPFs over radial distribution networks [16], [17], even in the multi-period case [18]. In order to preserve the convexity of the resulting SDP relaxation, constraint (6) is removed in (19). Although the solution thus obtained might not satisfy all the complementarity constraints in general, arguments similar to those presented in [11] can be used to show that the presence of the term $C_S(t)$ in the cost function (14) favors solutions with either $r_s^c(t) = 0$ or $r_s^d(t) = 0$, whenever this is possible. When the storage level $e_s(t)$ approaches the maximum capacity E_s, and further energy need be stored (e.g., due to high generation causing overvoltages), solutions featuring simultaneously $r_s^c(t) > 0$ and $r_s^d(t) > 0$ may actually arise. This can be explained as an attempt of the controller to draw energy from the network by taking advantage of the ESS round-trip efficiency $\eta_s^c \eta_s^d < 1$. In order to mitigate such an issue the following constraints can be added

$$e_s(\tau-1) + \eta_s^c r_s^c(\tau-1) \Delta T \leq E_s, \tag{20}$$

for $\tau \in \mathcal{T}$, with the purpose of forcing the controller to find a charging signal $r_s^c(t)$ which does not violate the ESS capacity E_s irrespective of the value of the discharging signal $r_s^d(t)$.

The solution of the resulting convex relaxation returns ESS control signals $r_s^{c*}(\tau-1)$, $r_s^{d*}(\tau-1)$, $b_s^*(\tau-1)$, and OLTC

$$\begin{aligned}
\min_{\substack{V_k(\tau), l(\tau-1), r_s^c(\tau-1) \\ r_s^d(\tau-1), b_s(\tau-1)}} \ & \sum_{\tau=t+1}^{t+H} C(\tau) + \gamma_T C_T(t+H) \qquad (19) \\
\text{s.t.} \quad & \\
& \underline{v}_1^2 \leq |V_1(\tau)|^2 \leq \overline{v}_1^2 \\
& \underline{v}_k^2 \leq |V_k(\tau)|^2 \leq \overline{v}_k^2 \\
& V_1(\tau) = V_1(\tau-1) + l(\tau-1) \\
& |l(\tau-1)|^2 \leq \overline{l}^2 \\
& e_s(\tau) = e_s(\tau-1) + \eta_s^c r_s^c(\tau-1) \Delta T - \frac{1}{\eta_s^d} r_s^d(\tau-1) \Delta T \\
& r_s^c(\tau-1) r_s^d(\tau-1) = 0 \\
& 0 \leq e_s(\tau) \leq E_s \\
& r_s(\tau-1) = r_s^c(\tau-1) - r_s^d(\tau-1) \\
& M_s \begin{bmatrix} r_s(\tau-1) \\ b_s(\tau-1) \end{bmatrix} \leq m_s \\
& r_s^c(\tau-1) \geq 0 \\
& r_s^d(\tau-1) \geq 0 \\
& \mathrm{Re}\big(V_i(\tau) \big[V_i(\tau) - V_j(\tau) \big]^* y_{ij}^* \big) \leq \overline{P}_{ij} \\
& \mathrm{Re}\Big(V_k(\tau) \sum_{j \in \mathcal{N}} V_j^*(\tau) Y_{kj}^* \Big) = P_k^G(\tau) - P_k^D(\tau) - r_k(\tau-1) \\
& \mathrm{Im}\Big(V_k(\tau) \sum_{j \in \mathcal{N}} V_j^*(\tau) Y_{kj}^* \Big) = Q_k^G(\tau) - Q_k^D(\tau) - b_k(\tau-1) \\
& k \in \mathcal{N}^L,\ s \in \mathcal{S},\ (i,j) \in \mathcal{E},\ \tau \in \mathcal{T}.
\end{aligned}$$

control signals $l^*(\tau-1)$, for $\tau \in \mathcal{T}$. The feasibility of such a solution for the original problem can be easily checked by solving a sequence of load flow problems over $\mathcal{T}$, in which the ESS and OLTC control signals are fixed to the values computed previously.

IV. Implementation

In this section, a receding horizon implementation of the proposed OLTC-ESS control strategy, as well as the approach taken for demand and generation forecasting, are discussed.

A. Receding horizon approach

In formulating problem (19), the active and reactive power demand $P_k^D(t+h)$, $Q_k^D(t+h)$, as well as the active and reactive power generation $P_k^G(t+h)$ and $Q_k^G(t+h)$, are supposed to be known over the whole control horizon $h = 1, \dots, H$. In practice, these values are replaced with their forecasts computed at time t, namely $\hat{P}_k^D(t+h|t)$, $\hat{Q}_k^D(t+h|t)$, $\hat{P}_k^G(t+h|t)$ and $\hat{Q}_k^G(t+h|t)$. Forecast inaccuracies inevitably introduce errors in the computation of the solution. One way to mitigate such an effect is to apply a receding horizon approach [19]. Roughly speaking, at time t problem (19) is solved based on the load and generation forecasts available at that time. Then, only the values $r_s^{c*}(t)$, $r_s^{d*}(t)$, $b_s^*(t)$ and $l^*(t)$ are applied. The same steps are repeated at the next time instants by exploiting the updated load and generation forecasts that become available.

The length H of the control horizon in (19) is tuned by trading-off conflicting objectives. On the one hand, H should be as large as possible in order to fully exploit the predictive capability of the model (e.g., discharging ESSs in advance when overvoltages are forecast). Moreover, the larger H, the more effective the operating policy in terms of minimizing line losses or ESS and OLTC usage. On the other hand, the length of the control horizon directly affects the computation time required to solve problem (19). Additionally, larger lead times clearly imply less accurate forecasts, and therefore less reliable control policies. A possible way to tune the parameter H is to select the largest value compatible with predefined computation time and prediction accuracy.

B. Demand and generation forecasting

Forecasting demand and generation at each bus of an LV network can be particularly challenging. In fact, in a typical LV network few quantities are measured, and those measurements are usually not available in real-time (they are transferred to data collectors in a batch way, e.g. monthly).

For the above reason, in this paper we take the approach to demand and generation forecasting proposed in [9]. Aggregate demand and generation forecasts are computed by exploiting suitable models estimated from historical data, and the (limited) real-time information available at the substation level. The actual demand and generation forecasts at each bus are then computed by distributing the aggregate predictions according to the estimated fraction of demand and generation pertinent to each bus. Notice that the proposed approach requires that only the MV/LV substation is equipped with a measurement station, providing real-time measurements of active power injected at the slack bus, as well as meteorological variables useful to predict generation from available renewable energy sources (e.g., solar irradiance and outdoor temperature in the case of photovoltaic generation).

V. Numerical results

The proposed OLTC-ESS control algorithm is tested using the topology and the demand and generation profiles of the Italian LV network considered in [18]. The test network consists of 17 buses, 26 loads and 4 photovoltaic units. For all loads and generators, three months of active and reactive power profiles are available with sampling time $\Delta T = 15$ min. Measurements of solar irradiance and outdoor temperature at the MV/LV substation are also available with the same resolution. These historical data sets are used to estimate the models of demand and generation described in [9]. We simulate the presence of two ESSs installed in the network at buses 7 and 11. These locations are determined by applying the siting procedure proposed in [18].

In problem (19), the choice $\underline{v}_k = 0.9$ pu and $\overline{v}_k = 1.1$ pu is made for $k \in \mathcal{N}^L$ in accordance with the European Norm 50160. The bounds $\overline{P}_{ij}$ on the real power flow are all set to 35 kW. For both ESSs, independent bounds on $r_s(t)$ and $b_s(t)$ are considered, in particular $|r_s(t)| \leq 15$ kW and $|b_s(t)| \leq 15$ kVar. Notice that these constraints can be expressed in the form (8). The desired state of charge at the end of a control horizon is set to 50%, i.e. $\xi = 0.5$ in (18). Values of charging and discharging efficiencies are $\eta_s^c = \eta_s^d = 0.95$. It is assumed that the number of tap positions is 17. Tap position 0 corresponds to the nominal voltage at the slack bus. A single tap change corresponds to a voltage variation $\Delta V = 0.01087$ pu. This implies that the signal $l(t)$ can take a finite number of values. A maximum of three tap changes are allowed at each time step, implying $\bar{l} = 3\Delta V$. To avoid solving a mixed integer program, in problem (19) voltage variations $l(t)$ at the slack bus are treated as continuous variables. The number of tap changes to be executed in a time step is then obtained by rounding off the value $l^*(t)/\Delta V$.

All the results presented hereafter are obtained by using the CVX modelling toolbox and the SeDuMi solver. Considering a control horizon $H = 8$ (corresponding to two hours), the SDP relaxation of problem (19) is solved in few seconds on a 3 GHz PC with 8 GB RAM. The optimal solutions of the SDP problems turn out to be always feasible for the original problem (19).

In the following sections we present two types of results. The first analysis is for fixed weights γ_S and γ_O and different ESS sizes. The second analysis is concerned with varying the weight γ_O while keeping the ESS sizes and the weight γ_S fixed. Performance of the proposed OLTC-ESS control algorithm is tested on two challenging days featuring both over- and undervoltages (see the blue profiles in the top of Fig. 1).

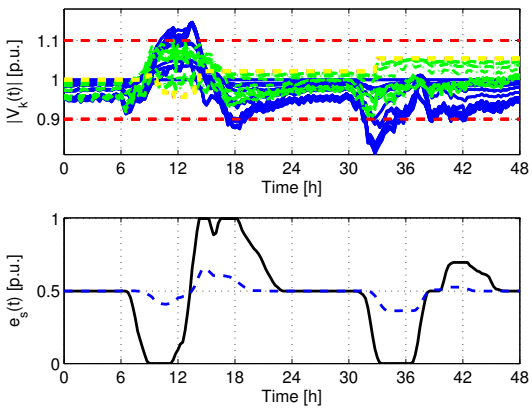

Fig. 1. Top: Voltage magnitudes at buses $k \in \mathcal{N}^L$ with (green dashed lines) and without (blue solid lines) OLTC-ESS control. The yellow dashed line refers to the voltage at the slack bus with OLTC-ESS control. Bottom: Storage levels $e_7(t)$ (black solid line) and $e_{11}(t)$ (blue dashed line).

A. Analysis with respect to ESS sizes

For the considered network and data set, the nominal ESS capacities returned by the sizing procedure in [18] are $E_7^* = 15$ kWh and $E_{11}^* = 55$ kWh. In this section we consider three scenarios where the ESS sizes are chosen to be 25%, 50% and 75% of their nominal values. The weights in (14) are set to $\gamma_S = 0.015$ and $\gamma_O = 0.05$ kWh/V^2. The weight γ_T in (19) depends on the total installed ESS capacity according to the formula $\gamma_T = 6.75 \cdot 10^3 / \sum_{s \in \mathcal{S}} E_s$.

Without the use of the OLTC, voltage problems cannot be solved in any of the three scenarios. In particular, violations of the voltage bounds are unacceptable both in magnitude and duration. On the other hand, when the OLTC is used, voltage problems are avoided in most cases and when this is not the case (due to inaccurate forecasts, discretization of the OLTC command, etc.) voltage violations are negligible, as can be observed in the top of Fig. 1, corresponding to the case $E_s = 0.5E_s^*$.

The usage of the OLTC and the corresponding voltage profile at the slack bus under the three scenarios are shown in Fig. 2. It can be observed that, as the ESS sizes are decreased, the frequency of the tap changes increases. On average, the OLTC is used every 6 hours in the case $E_s = 0.75E_s^*$, every 3.5 hours in the case $E_s = 0.5E_s^*$ and every 2 hours in the case $E_s = 0.25E_s^*$. Moreover, also the average magnitude of the OLTC command $l(t)$ increases as the ESS sizes are decreased. In the case $E_s = 0.25E_s^*$, the voltage at the slack bus spans almost the whole range of variation allowed. This is done in order to compensate for the limited ESS capacity. In general, it turns out that the OLTC is operated when the level of at least one ESS is at its minimum or maximum, see, e.g., Fig. 1.

B. Analysis with respect to OLTC weighting

In this section we fix the ESS sizes at 50% of their nominal values. The weights γ_S and γ_T are as above, while the weight γ_O takes the values 0.025, 0.05 and 0.25 kWh/V^2, to simulate different weighting of the OLTC actions. This analysis is carried out to determine the most satisfactory trade off between OLTC and ESS usage. Indeed, increasing γ_O implies that the number and magnitude of tap changes decreases, while more stress is put on the ESSs. For instance, in the left-hand side of Fig. 3 one can observe how the usage of the ESS at bus 11 grows between hour 6 and hour 18 as the OLTC usage is more penalized. In the same time interval the OLTC usage decreases as expected while increasing γ_O.

VI. Conclusions

In this paper, a control strategy for the coordinated operation of OLTC and ESSs deployed in a distribution network has been proposed. The joint operation control law is obtained by formulating an optimization problem, which makes it possible to account for real losses, ESS usage and state of charge, and OLTC interventions. Moreover, a receding horizon approach is adopted which allows one to cope with uncertainties arising during operation and due to the scarce availability of on-line measurements in LV networks. The devised strategy has been tested on real data from a section of an Italian LV feeder. The obtained numerical results show several interesting features with specific reference to understanding the potential of the OLTC to alleviate the voltage support task of ESS and vice versa.

Ongoing work is devoted to a more detailed description of uncertainties arising during operation, possibly based on scenario analysis and probabilistic forecast approaches.

References

[1] A. T. Procopiou, C. Long, and L. F. Ochoa, "Voltage control in LV networks: An initial investigation," in *Proc. of 5th IEEE/PES Innovative Smart Grid Technologies Europe*, 2014, pp. 1–6.

[2] F. A. Viawan, A. Sannino, and J. Daalder, "Voltage control with on-load tap changers in medium voltage feeders in presence of distributed generation," *Electric Power Systems Research*, vol. 77, no. 10, pp. 1314–1322, 2007.

[3] C. Long and L. F. Ochoa, "Voltage control of PV-rich LV networks: OLTC-fitted transformer and capacitor banks," *IEEE Transactions on Power Systems*, vol. 31, no. 5, pp. 4016–4025, 2016.

[4] A. Kulmala, S. Repo, and P. Järventausta, "Coordinated voltage control in distribution networks including several distributed energy resources," *IEEE Transactions on Smart Grid*, vol. 5, no. 4, pp. 2010–2020, 2014.

[5] U.S. DOE, "Grid energy storage," [Online]. Available: http://energy.gov/oe/downloads/grid-energy-storage-december-2013 (accessed Nov. 7, 2016), 2013.

[6] M. Zidar, P. S. Georgilakis, N. D. Hatziargyriou, T. Capuder, and D. Škrlec, "Review of energy storage allocation in power distribution networks: applications, methods and future research," *IET Generation, Transmission & Distribution*, vol. 10, no. 3, pp. 645–652, 2016.

[7] X. Liu, A. Aichhorn, L. Liu, and H. Li, "Coordinated control of distributed energy storage system with tap changer transformers for voltage rise mitigation under high photovoltaic penetration," *IEEE Transactions on Smart Grid*, vol. 3, no. 2, pp. 897–906, 2012.

[8] P. Wang, D. H. Liang, J. Yi, P. F. Lyons, P. J. Davison, and P. C. Taylor, "Integrating electrical energy storage into coordinated voltage control schemes for distribution networks," *IEEE Transactions on Smart Grid*, vol. 5, no. 2, pp. 1018–1032, 2014.

[9] D. Zarrilli, A. Giannitrapani, S. Paoletti, and A. Vicino, "Energy storage operation for voltage control in distribution networks: A receding horizon approach," *IEEE Transactions on Control Systems Technology*, vol. PP, no. 99, pp. 1–11, 2017.

[10] J. J. Grainger and W. D. Stevenson, *Power system analysis*. McGraw-Hill, 1994.

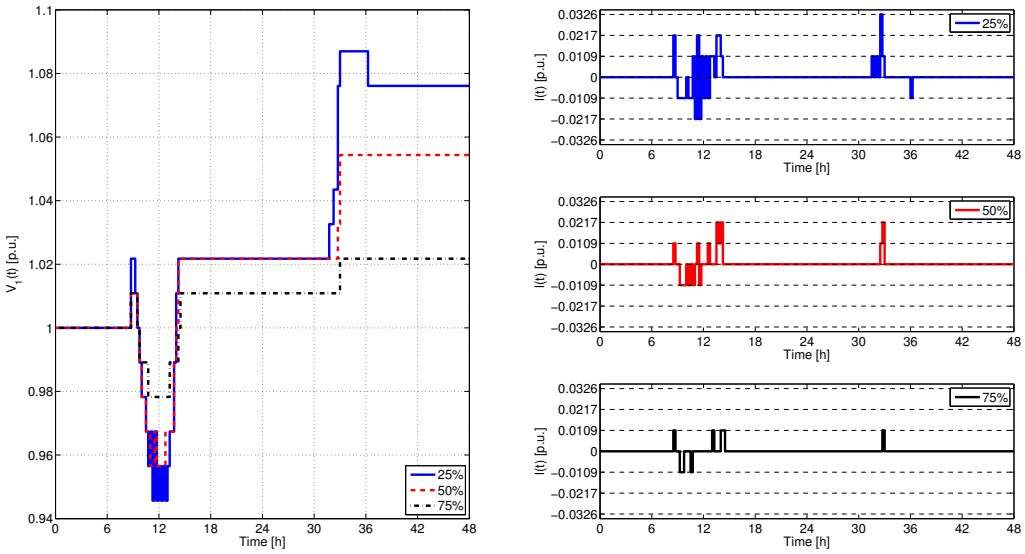

Fig. 2. OLTC operation for different values of the installed storage capacity. Left: Voltage magnitude at the slack bus. Right: OLTC command $l(t)$.

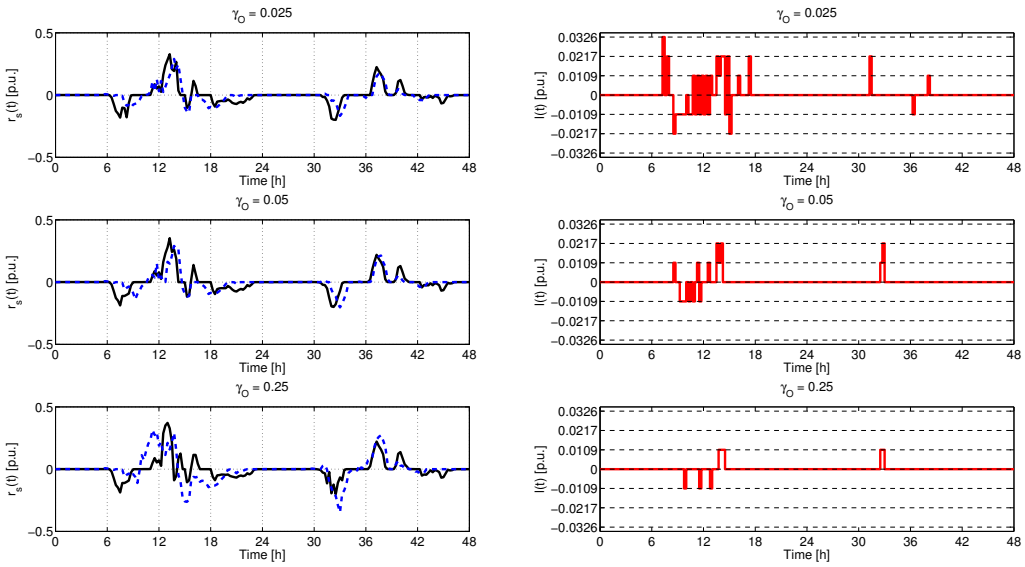

Fig. 3. OLTC-ESS operation for ESS capacities $E_s = 0.50E_s^*$ and different values of parameter γ_O. Left: ESS active power $r_7(t)$ (black solid line) and $r_{11}(t)$ (blue dashed line). Right: OLTC command $l(t)$.

[11] S. Gill, I. Kockar, and G. W. Ault, "Dynamic optimal power flow for active distribution networks," *IEEE Transactions on Power Systems*, vol. 29, no. 1, pp. 121–131, 2014.

[12] M. Nick, R. Cherkaoui, and M. Paolone, "Optimal allocation of dispersed energy storage systems in active distribution networks for energy balance and grid support," *IEEE Transactions on Power Systems*, vol. 29, no. 5, pp. 2300–2310, 2014.

[13] J. Lavaei and S. H. Low, "Zero duality gap in optimal power flow problem," *IEEE Transactions on Power Systems*, vol. 27, no. 1, pp. 92–107, 2012.

[14] D. Gayme and U. Topcu, "Optimal power flow with large-scale storage integration," *IEEE Transactions on Power Systems*, vol. 28, no. 2, pp. 709–717, 2013.

[15] S. H. Low, "Convex relaxation of optimal power flow – Part I: Formulations and equivalence," *IEEE Transactions on Control of Network Systems*, vol. 1, no. 1, pp. 15–27, 2014.

[16] L. Gan and S. H. Low, "Convex relaxations and linear approximation for optimal power flow in multiphase radial networks," in *Proc. of 18th Power Systems Computation Conference*, 2014, pp. 1–9.

[17] S. H. Low, "Convex relaxation of optimal power flow – Part II: Exactness," *IEEE Transactions on Control of Network Systems*, vol. 1, no. 2, pp. 177–189, 2014.

[18] A. Giannitrapani, S. Paoletti, A. Vicino, and D. Zarrilli, "Optimal allocation of energy storage systems for voltage control in LV distribution networks," *IEEE Transactions on Smart Grid*, vol. PP, no. 99, pp. 1–12, 2016.

[19] J. M. Maciejowski, *Predictive control with constraints*. Pearson Education, 2002.